Inhibitor screening of Spike variants reveals the heterogeneity of neutralizing antibodies to COVID-19 infection and vaccination

Xiaomei Zhang[1,8], Mei Zheng[2,3,5,8], Te Liang[1,8], Haijian Zhou[4,5,8], Hongye Wang[1], Jiahui Zhang[1], Jing Ren[1], Huoying Peng[1], Siping Li[1], Haodong Bian[1], Chundi Wei[1], Shangqi Yin[2,3,5], Chaonan He[2,3,5]. Ying Han[2,3,5], Minghui Li[4,5], Xuexin Hou[4,5], Jie Zhang[6], Liangzhi Xie[6], Jing Lv[7], Biao Kan[4,5,9], Yajie Wang[2,3,5,9], Xiaobo Yu[1,9]

Affiliations

[1] State Key Laboratory of Proteomics, Beijing Proteome Research Center, National Center for Protein Sciences-Beijing (PHOENIX Center), Beijing Institute of Lifeomics, Beijing, 102206, China.

[2] Department of Clinical Laboratory, Beijing Ditan Hospital, Capital Medical University, Beijing, China.

[3] Department of Research Ward, Beijing Ditan Hospital, Capital Medical University, Beijing, China.

[4] State Key Laboratory of Infectious Disease Prevention and Control, National Institute for Communicable Disease Control and Prevention, Chinese Center for Disease Control and Prevention, Beijing, 102206, China

[5] Joint Laboratory for Pathogen Identification of ICDC and Ditan Hospital, Beijing, 102206, China

[6] Beijing Key Laboratory of Monoclonal Antibody Research and Development, Sino Biological, Inc., Beijing, 100176, China

[7] Gobond Testing Technology (Beijing) Co., Ltd., Beijing, 102629, China.

[8] These authors contributed equally to this work.

[9] Correspondence: xiaobo.yu@hotmail.com (X. Y.), wangyajie@ccmu.edu.cn (Y. W.), kanbiao@icdc.cn (B. K.)

Highlights

- Developed a high throughput assay to screen the neutralizing effect of antibodies across multiple SARS-CoV-2 Spike variants simultaneously.
- Characterized the heterogeneity of neutralizing antibodies produced in response to COVID-19 infection and vaccination.
- Demonstrated the capacity of Spike variants neutralization is associated with the diversity of anti-Spike antibodies.

Abstract

Mutations of the coronavirus responsible for coronavirus disease 2019 (COVID-19) could impede drug development and reduce the efficacy of COVID-19 vaccines. Here, we developed a multiplexed Spike-ACE2 Inhibitor Screening (mSAIS) assay that can measure the neutralizing effect of antibodies across numerous variants of the coronavirus's Spike (S) protein

simultaneously. By screening purified antibodies and serum from convalescent COVID-19 patients and vaccinees against 72 S variants with the mSAIS assay, we identified new S mutations that are sensitive and resistant to neutralization. Serum from both infected and vaccinated groups with a high titer of neutralizing antibodies (NAbs) displayed a broader capacity to neutralize S variants than serum with low titer NAbs. These data were validated using serum from a large vaccinated cohort (n=104) with a tiled S peptide microarray. In addition, similar results were obtained using a SARS-CoV-2 pseudovirus neutralization assay specific for wild-type S and four prevalent S variants (D614G, B.1.1.7, B.1.351, P.1), thus demonstrating that high antibody diversity is associated with high NAb titers. Our results demonstrate the utility of the mSAIS platform in screening NAbs. Moreover, we show that heterogeneous antibody populations provide a more protective effect against S variants, which may help direct COVID-19 vaccine and drug development.

Keywords

SARS-CoV-2, COVID-19, microarray, neutralizing antibody, mutation, Spike

Introduction

Coronavirus disease 2019 (COVID-19) is caused by the severe respiratory coronavirus 2 (SARS-CoV-2). As of May 2021, SARS-CoV-2 had infected 162 million people and caused over three million deaths worldwide (Dong et al.,

2020). A key step in infection is viral entry, which is facilitated by the interaction between the SARS-CoV-2 Spike (S) protein via its receptor binding domain (RBD) (319 – 541 aa) with the human Angiotensin-Converting Enzyme 2 (ACE2) receptor. Thus, this interaction is a major focus in drug and vaccine development efforts (Burki, 2021; Dai and Gao, 2021). For example, the current COVID-19 vaccines approved by the U.S. Food and Drug Administration (FDA) stimulate the immune response to generate antibodies capable of neutralizing the Spike-ACE2 interaction. Unfortunately, SARS-CoV-2 is mutating, with new variants emerging nearly every week that could impede drug development and reduce the efficacy of COVID-19 vaccines (Dai and Gao, 2021; Kemp et al., 2021).

Mutations in the S protein are of particular concern since they could enable SARS-CoV-2 to evade defense mechanisms that are elicited by COVID-19 vaccines and therapeutic antibodies (Aschwanden, 2021; Del Rio and Malani, 2021). For example, the D614G variant, which was first identified in July 2020, has a faster infection rate and higher viral load in the upper respiratory tract than the wild-type “Wuhan-Hu-1” strain (Hou et al., 2020b; Korber et al., 2020). It has since become one the most prevalent strains. The B.1.1.7 variant (D614G, N501Y) is more infectious and may lead to increased mortality compared to the parental strain (Davies et al., 2021; Galloway et al., 2021). The B.1.351 and P.1 variants contain three RBD mutations at E484K, N501Y, and K417N or K417T, respectively. These mutations have shown

89 resistance to neutralizing antibodies (NAbs) produced by convalescent
90 COVID-19 patients and vaccinees that inhibit the wild-type Spike-ACE2
91 interaction (Garcia-Beltran et al., 2021; Liu et al., 2021; Madhi et al., 2021;
92 Wang et al., 2021a; Wang et al., 2021b; Wibmer et al., 2021). The vaccinees in
93 these studies received the most popular vaccines worldwide, including
94 mRNA-based COVID-19 vaccines (Moderna and Pfizer BioNTech) and a
95 replication-deficient chimpanzee adenoviral vector COVID-19 vaccine
96 (AstraZeneca). Similar results were obtained when testing a B.1.1.7 variant
97 with an additional E484K mutation (Collier et al., 2021; Wang et al., 2021b).
98 These studies highlight the importance of an assay that can measure the
99 humoral response to S variants in developing effective therapeutic antibodies
100 and vaccines for COVID-19 (Burki, 2021; Priesemann et al., 2021).

101 To address this urgent need, we developed a protein microarray for the
102 high throughput, multiplexed detection of NAbs to SARS-CoV-2 S variants.
103 This multiplexed Spike-ACE2 Inhibitor Screening (mSAIS) assay is simple to
104 use, able to detect NAbs to numerous S variants simultaneously, requires
105 minimal sample volume (i.e., 20 µL serum), and can be performed with
106 common laboratory equipment. It could also be used with other potential
107 neutralizing molecules (e.g., small molecules). To demonstrate the potential of
108 the mSAIS assay, we assessed the neutralization potential of purified anti-S
109 antibodies and serum from convalescent COVID-19 patients and vaccinees
110 across 72 S variants. The sensitivity and resistance of the various S protein

mutations to the NAbs were determined, and new escape mutations that are not targeted by vaccine-induced antibodies were identified**.** The neutralization capacity of high and low titer NAb titer samples was also compared. Our results were validated using a peptide-based microarray and SARS-CoV-2 pseudovirus neutralization assay.

Results

Development of the mSAIS assay.

The mSAIS assay enables the simultaneous screening of various potential neutralizing molecules across numerous SARS-CoV-2 S variants within 2 hours (Figure 1A). Here, 72 S protein variants with a polyhistidine tag at the C-terminus were expressed in the human embryonic kidney 293 (HEK293) cell line (Figure S1), purified, and printed onto a chemically-modified glass slide as previously described (Wang et al., 2020; Zhang et al., 2020b). The printed S protein variants were selected from the COVID-19 virus mutation tracker database (Figure S2) and literature, and included 2 variants with mutations in the S protein's subunit 1 (S1) and subunit 2 (S2) domains, 7 variants with mutations in S1, and 63 variants with mutations in the RBD (Alam et al., 2021). Prevalent SARS-CoV-2 strains, such as the D614G, B.1.1.7, and B.1.351 strains, were among the variants printed. In addition, two negative controls and one positive control (SARS-CoV-2 wild-type RBD) were printed on the array (Figure S3). The negative controls included on the array were the

SARS-CoV-2 Nucleocapsid (N) protein and the RBD of the Middle East respiratory syndrome coronavirus 2 (MERS-CoV-2). Following printing, the sample (e.g., NAb) and a Cy5-labeled extracellular domain of ACE2 were sequentially incubated on the array with alternated wash steps to remove unbound sample and ACE2. Thus, S-ACE2 complex formation resulted in fluorescence whereas neutralizing samples decreased fluorescence.

Before using the mSAIS assay to screen samples, the reproducibility of the array and the binding of the S variants with ACE2 in the presence and absence of NAbs were evaluated. The results show that the intra- and inter-array *r* correlations for each step of the assay were 0.99 and 0.98, respectively (Figure S4, Figure 1B and 1C). Furthermore, the neutralizing capacity of 13 serum samples from vaccinees determined by the mSAIS assay was compared to the data obtained using the live SARS-CoV-2. The *r* correlation between the two approaches was 0.82 (Figure S5), demonstrating that the mSAIS assay has high reproducibility and is a feasible approach for screening potential neutralizing molecules. It is also important to note that working with live SARS-CoV-2 requires biosafety level 3 (BSL3) facilities whereas the mSAIS assay can be performed safely at BSL1 or BSL2 depending on the nature of the tested samples.

Characterizing ACE2 interactions with Spike variants with the mSAIS assay

By testing different amounts of purified antibodies or serum, the half maximal inhibitory concentration (IC50) or effective concentration (EC50) can be determined, respectively, and the results visualized via fluorescence. When the concentration of ACE2 applied to the assay was low (≤ 2.5 µg/mL), the fluorescent signal across the different S variants varied, thus indicating that the binding affinities of ACE2 to the S variants are not the same (Figure 2A). Indeed, the calculation of the EC50 for the S variants with mutations between residues 234 - 614 shows that the binding affinity (EC50) ranges from 0.65 to 17.25 µg/mL. ACE2 had the lowest binding affinity to two S variants, F465E and N487R, with an EC50 of 16.16 and 17.25 µg/mL, respectively (Figure 2B).

The EC50 ratios between the wild-type and variant S proteins were calculated and log2 transformed (Figure 2C). Using a 2-fold minimum as the selection criteria, 10 mutations that weaken the S-ACE2 interaction were identified, including A372T, F377L, G446V, F456E, G485S, F486S, N487R, F490L, P499R and Y505C (Figure 2C and 2D). Notably, the S variant D614G did not appear to affect ACE2 binding, which agrees with a previous study using surface plasmon resonance (Zhang et al., 2020a).

Interestingly, 8/10 (80%) mutations that decreased the ability of the S protein to bind ACE2 (G446V, F456E, G485S, F486S, N487R, F490L, P499R, Y505C) are located at the RBD-ACE2 interaction interface (Figure 2E). Moreover, F456E and N487R had the weakest ACE2 binding affinities. These results further support the importance of the RBD domain in antibody

177 neutralization (Barnes et al., 2020; Dai and Gao, 2021; Tan et al., 2020).

178

179 **Heterogeneous reaction of antibodies to Spike variants**

180 Three antibodies that bind to the S protein's RBD (Figure S6) were tested with
181 the mSAIS assay, including a mouse monoclonal antibody #73, a rabbit
182 polyclonal antibody #21, and a rabbit monoclonal antibody #53 (Figure 3). The
183 IC50 of antibodies #21 and #53 to the S variants range from 42.04 – 10,000
184 ng/mL and 0.00063 – 10,000 ng/mL, respectively (Figure 3B and 3C). However,
185 antibody #73 did not inhibit the RBD-ACE2 interaction (Figure 3A), indicating
186 that not all anti-RBD antibodies have neutralizing activity.

187 Antibody #21 was unable to neutralize the formation of the S-ACE2
188 complex for 8 "resistant" S variants: R408I, HV69-70 deletion/N501Y/D614G
189 (B.1.1.7 strain), G446V, F456E, N487R, F490L, Y505C, and
190 K417N/E484K/N501Y (B.1.351 strain) (Figure 3B). Two other studies also
191 observed similar results for the B.1.351 strain (Li et al., 2021; Wang et al.,
192 2021a). Using a two-fold difference in signal compared to the wild-type S
193 protein as the criteria, 33 variants showed resistance to neutralization with
194 antibody #21(Figure 3D). Seventeen of the 33 (51.5%) mutations are located
195 between residues 437 and 508, which is the region of the RBD that physically
196 interacts with ACE2 (Singh et al., 2021) (Figure 3D and 3F, Figure S7A). Four
197 of the ten (40%) sensitive mutations are also located within the RBD interface
198 (Figure 3D and 3F, Figure S7A).

Antibody #53 had 13 escape mutations of varying resistance, with 5 mutations (F456E, F486S, N487R, N501Y, Y505C) showing complete resistance to neutralizing activity (Figure 3C and 3E). Seven (53.85%) mutations are located within the interface of the RBD-ACE2 interaction (Figure 3E and 3G, Figure S7B). Interestingly, six (46.15%) sensitive mutations are not located within the RBD-ACE2 interface (Figure 3E and 3G, Figure S7B), which indicates that binding to non-RBD binding epitopes can also have neutralization effects (Li et al., 2020; Prevost and Finzi, 2021).

Heterogeneous reaction of serological NAbs to S variants in convalescent COVID-19 patients

We next screened the serum from 25 COVID-19 patients who had recovered from SARS-CoV-2 infection. Using hierarchical cluster analysis, the convalescent patients clustered into three groups based on their NAb titers: high, low, and mixed (Figure 4A and 4B). After determining the percentage of escape mutations under three different EC50 thresholds (10, 30, 50), it was observed that the number of escape mutations were fewer for the high-titer NAb group than the low-titer NAb group (Figure 4C).

Next, the NAbs to wild-type and mutant S proteins were compared (Figure 4D). The D614G variant did not lead to a change of NAbs to S1 and S1+S2 proteins (Figure 4E, Figure S8). Using statistical analysis, the number of NAbs to eight mutated proteins was significantly decreased, including 4 known

escape mutations [K417N, G446V, F490L, K417N/E484K/N501Y (B.1.351 strain)] and 4 newly identified escape mutations (A372S, F456E, N487R, Y505C) (Figure 4F and 4G) (Chen et al., 2021; Li et al., 2021; Li et al., 2020; Zhou et al., 2021). Notably, structural analyses show that 5 escape mutations (K417N/E484K/N501Y, G446V, F456E, N487R, F490L) are located within the interface of RBD-ACE2 interaction, thus indicating that this RBD subdomain is important in neutralizing SARS-CoV-2 infection (Wang et al., 2020). All these results demonstrate the heterogeneous reactivity of NAbs produced by COVID-19 patients across S variants.

Heterogeneous reactivity of NAbs produced by vaccinees to S variants

The mSAIS assay was next used to measure the neutralizing effect of antibodies produced by 30 vaccinees who received the inactivated vaccine in China (Wu et al., 2021). NAbs were generated to the majority of S variants (Figure 5A). Using hierarchical cluster analysis, the vaccinees consistently clustered into two groups based on the level of their NAb titer: low and high (Figure 5A and 5B). Using three EC50 thresholds (10, 20, 30), high-titer NAb group had a lower number of escape mutations compared to low-titer NAb group (Figure 5C).

Next, the NAb titers of vaccinees across all S variants were ascertained (Figure 5D). Like the convalescent COVID-19 patients, the D614G variant did not alter the neutralizing effect of the NAbs compared to wild-type S1+S2, S2,

and RBD (Figure 5E, Figure S9). Using statistical analysis, four escape mutations were identified, including 2 known (N501Y, K417N/E484K/N501Y) and 2 new (K378N, P499R) mutations (Figure 5F and 5G) (Chen et al., 2021).

To validate the results obtained with the mSAIS assay, we analyzed the NAbs with a SARS-CoV-2 pseudovirus neutralization assay displaying wild-type and mutant S (wild-type, D614G, B.1.1.7, B.1.351, P.1). The results for the D614G, B.1.1.7, B.1.351 variants aligned with the data obtained with the mSAIS assay (Figure 5H). The vaccinees also separated into high- and low-titer NAb groups (Figure 5I), further supporting the data obtained with the mSAIS assay Figure 5C).

High titer of NAbs contain anti-Spike antibodies with diverse binding epitopes

Two recent studies with rhesus macaques have shown that a high titer of NAbs produced in response to vaccination (DNA-based or adenovirus serotype 26 (Ad26) vector-based) provided good protection against infection when challenged with SARS-CoV-2 (Mercado et al., 2020; Yu et al., 2020). In another study, NAb titers were significantly higher in vaccinees who had COVID-19 previously than vaccinees who never had COVID-19. Moreover, the vaccinees who had been infected with SARS-CoV-2 possessed NAbs that were able to neutralize all prevalent S variants (Stamatatos et al., 2021).

In order to provide insight into how well the high-titer NAb samples could protect against SARS-CoV-2 variants, we analyzed the differential expression of anti-S antibodies in the vaccinees. The level of antibodies that target the S protein's S1, S2 extracellular domain (ECD), and RBD is higher in the high-titer NAb group than the low-titer NAb group. Of these three antibodies, the differing level of anti-RBD antibodies across the two groups was the most pronounced (Figure 6A).

Next, we performed epitope mapping of the vaccinees' serological anti-S antibodies using a tiled peptide microarray representing the full-length S protein as previously described (Liang et al., 2021; Wang et al., 2020). Indeed, the results indicate that the high-titer NAb group bound to more diverse epitopes than the low-titer NAb group (Figure 6B). The number of immunogenic peptides within the S1, S2ECD, and RBD is also consistently higher in the high-titer NAb group (Figure 6C).

To further validate our findings, sera from the 104 vaccinees were analyzed using a SARS-CoV-2 pseudovirus neutralization assay. Prior to data analysis, all vaccinees were separated into three groups according to their NAb titers (<10, 10-50, >50). Notably, the results show that the concentration of anti-S antibodies is proportional to the concentration of NAbs. However, there was no difference in the levels of anti-S1 antibodies that target the N-terminus or C-terminus across the vaccinees. The levels of anti-S2 ECD antibodies were significantly different only between NAb titers of <10 and >50

(Figure 7A). These results demonstrate that the antibodies produced in response to vaccination of inactivated vaccine primarily target the RBD (Figure 6A and 7A).

The peptide microarray was also employed to examine serological NAbs with a larger vaccinated cohort (n=104). The data confirm that the anti-S antibodies in the high-titer NAb group bind to more peptides representing the S1, S1 N-terminal domain, RBD, and S2 ECD of the S protein than the low-titer NAb group (Figure 7B, 7C). These data indicate that high NAb titers contain anti-S antibodies with increased binding diversity.

Discussion

The SARS-CoV-2 virus has mutated over time, resulting in circulating viral strains with altered transmission efficiencies, mortality rates, and S variants that can escape from the neutralizing effect of antibodies (Alam et al., 2021) (Davies et al., 2021; Hou et al., 2020b; Prevost and Finzi, 2021). Therefore, significant effort has been devoted to improve the diagnosis, prevention, and treatment of COVID-19 patients infected with SARS-CoV-2 variants (Abdool Karim and de Oliveira, 2021).

In this work, we developed an mSAIS assay that enables the detection of NAbs to numerous S variants simultaneously and rapidly. It has numerous advantages compared to the enzyme-linked immunosorbent assay (ELISA) and pseudovirus neutralization assays (Li et al., 2021; Tan et al., 2020;

Weisblum et al., 2020). First, our flexible platform can be easily adapted to include new S variants as they emerge. Second, only a laser scanner capable of detecting Cy5 is required to perform the mSAIS assay. Third, the multiplexed nature of the platform significantly reduces the sample volume, reagents, time, and cost to obtain data compared to single-plexed assays (Xu et al., 2020). For example, only 20 µL of serum was needed to screen for NAbs against 72 S variants in this study. In comparison, the volume requirements for ELISA or the pseudovirus neutralization assay would be 1,440 (72×) or 3,240 (162×) µL, respectively.

Using the mSAIS assay, we compared purified mouse and rabbit antibodies. Of the three antibodies tested, antibody #53 was able to inhibit the S-ACE2 interaction across the most S variants, thus it is a superior candidate for COVID-19 therapy. The comprehensive mapping of antibodies to different S variants would be valuable in understanding the sensitivity of mutations to antibody neutralization, and help develop antibody cocktails for COVID-19 therapy (Li et al., 2021; Li et al., 2020; Prevost and Finzi, 2021; Starr et al., 2021).

Using serum from convalescent COVID-19 patients and vaccinees with the mSAIS assay, we identified 4 and 2 new resistant mutations, respectively, that escape NAb recognition (Figures 4 and 5). We also show that there are fewer escape mutations in high NAb titers than low titers, and this was observed in both convalescent COVID-19 patients and vaccinees (Figures 4C

and 5C). Using a large cohort of 104 vaccinees with multiple assays (i.e., mSAIS assay, peptide array, pseudovirus neutralization assay), we further demonstrate that high titer NAbs contain anti-S antibodies that target more diverse binding epitopes, thus leading to more neutralizing capacity across a breadth of S variants (Figure 6 and 7). The production of heterogenous antibodies could be due to the somatic mutations that occur during antibody maturation (Muecksch et al., 2021). Finally, our data suggest that an effective COVID-19 vaccination strategy to defend against the mutating SARS-CoV-2 is to elicit the immune response to produce high-titer NAbs that contain a large diversity of anti-S antibodies (Stamatatos et al., 2021; Starr. et al., 2021). However, the association between NAb titer and its ability to protect against SARS-CoV-2 infection in humans is unclear (Jin et al., 2021).

There were several limitations in this study. First, the mSAIS assay is *in vitro*, which might not accurately reflect results *in vivo*. Second, some conformational and glycosylation epitopes might not be detected using the peptide microarray that employed chemically-synthesized peptides (Wang et al., 2020). Finally, the number of serum samples from convalescent COVID-19 patients and vaccinees were limited. The results obtained in this study should be validated in a large different cohort in the future.

Conclusion

Altogether, we developed a high-throughput microarray-based mSAIS assay,

352 which enables the multiplexed and rapid screening of NAbs to SARS-CoV-2 S
353 variants. Using the mSAIS assay, we confirmed the neutralization capabilities
354 of NAbs to known mutations, identified a number of new mutations that are
355 resistant to the NAbs, and showed that there were fewer escape mutations
356 with high NAb titers than low NAb titers in both convalescent COVID-19
357 patients and vaccinees. The data demonstrate the great potential of our
358 proteomics platform in mapping the ability of NAbs to block the interaction
359 between SARS-CoV-2 S variants and ACE2 interactions. Although we tested
360 purified antibodies and serum in this study, the mSAIS assay could be used
361 with other sample types as well. Data gleaned from the mSAIS will help
362 develop more effective vaccines and therapeutic antibodies to fight against
363 COVID-19.

364

365 ## References

366 Abdool Karim, S.S., and de Oliveira, T. (2021). New SARS-CoV-2 Variants - Clinical, Public Health,
367 and Vaccine Implications. N Engl J Med *384*,1866-1868.
368 Alam, I., Radovanovic, A., Incitti, R., Kamau, A.A., Alarawi, M., Azhar, E.I., and Gojobori, T. (2021).
369 CovMT: an interactive SARS-CoV-2 mutation tracker, with a focus on critical variants. Lancet Infect Dis
370 *21*,602.
371 Aschwanden, C. (2021). Five reasons why COVID herd immunity is probably impossible. Nature *591*,
372 520-522.
373 Barnes, C.O., Jette, C.A., Abernathy, M.E., Dam, K.A., Esswein, S.R., Gristick, H.B., Malyutin, A.G., Sharaf,
374 N.G., Huey-Tubman, K.E., Lee, Y.E., *et al.* (2020). SARS-CoV-2 neutralizing antibody structures inform
375 therapeutic strategies. Nature *588*, 682-687.
376 Burki, T. (2021). Understanding variants of SARS-CoV-2. Lancet *397*, 462.
377 Chen, R.E., Zhang, X., Case, J.B., Winkler, E.S., Liu, Y., VanBlargan, L.A., Liu, J., Errico, J.M., Xie, X.,
378 Suryadevara, N., *et al.* (2021). Resistance of SARS-CoV-2 variants to neutralization by monoclonal and
379 serum-derived polyclonal antibodies. Nat Med *27*,717-726.
380 Collier, D.A., De Marco, A., Ferreira, I., Meng, B., Datir, R., Walls, A.C., Kemp, S.S., Bassi, J., Pinto, D.,
381 Fregni, C.S., *et al.* (2021). Sensitivity of SARS-CoV-2 B.1.1.7 to mRNA vaccine-elicited antibodies.

Nature *593*,136-141.

Dai, L., and Gao, G.F. (2021). Viral targets for vaccines against COVID-19. Nat Rev Immunol *21*, 73-82.

Davies, N.G., Jarvis, C.I., Group, C.C.-W., Edmunds, W.J., Jewell, N.P., Diaz-Ordaz, K., and Keogh, R.H. (2021). Increased mortality in community-tested cases of SARS-CoV-2 lineage B.1.1.7. Nature *593*,270-274.

Del Rio, C., and Malani, P. (2021). COVID-19 in 2021-Continuing Uncertainty. JAMA *325*,1389-1390.

Dong, E., Du, H., and Gardner, L. (2020). An interactive web-based dashboard to track COVID-19 in real time. Lancet Infect Dis *20*, 533-534.

Galloway, S.E., Paul, P., MacCannell, D.R., Johansson, M.A., Brooks, J.T., MacNeil, A., Slayton, R.B., Tong, S., Silk, B.J., Armstrong, G.L., *et al.* (2021). Emergence of SARS-CoV-2 B.1.1.7 Lineage - United States, December 29, 2020-January 12, 2021. MMWR Morb Mortal Wkly Rep *70*, 95-99.

Garcia-Beltran, W.F., Lam, E.C., St Denis, K., Nitido, A.D., Garcia, Z.H., Hauser, B.M., Feldman, J., Pavlovic, M.N., Gregory, D.J., Poznansky, M.C., *et al.* (2021). Multiple SARS-CoV-2 variants escape neutralization by vaccine-induced humoral immunity. Cell *184*,2372-2383.e9.

Hou, X., Zhang, X., Wu, X., Lu, M., Wang, D., Xu, M., Wang, H., Liang, T., Dai, J., Duan, H., *et al.* (2020a). Serum Protein Profiling Reveals a Landscape of Inflammation and Immune Signaling in Early-stage COVID-19 Infection. Mol Cell Proteomics *19*, 1749-1759.

Hou, Y.J., Chiba, S., Halfmann, P., Ehre, C., Kuroda, M., Dinnon, K.H., 3rd, Leist, S.R., Schafer, A., Nakajima, N., Takahashi, K., *et al.* (2020b). SARS-CoV-2 D614G variant exhibits efficient replication ex vivo and transmission in vivo. Science *370*, 1464-1468.

Jin, P., Li, J., Pan, H., Wu, Y., and Zhu, F. (2021). Immunological surrogate endpoints of COVID-2019 vaccines: the evidence we have versus the evidence we need. Signal Transduct Target Ther *6*, 48.

Kemp, S.A., Collier, D.A., Datir, R.P., Ferreira, I., Gayed, S., Jahun, A., Hosmillo, M., Rees-Spear, C., Mlcochova, P., Lumb, I.U., *et al.* (2021). SARS-CoV-2 evolution during treatment of chronic infection. Nature *592*,277-282.

Korber, B., Fischer, W.M., Gnanakaran, S., Yoon, H., Theiler, J., Abfalterer, W., Hengartner, N., Giorgi, E.E., Bhattacharya, T., Foley, B., *et al.* (2020). Tracking Changes in SARS-CoV-2 Spike: Evidence that D614G Increases Infectivity of the COVID-19 Virus. Cell *182*, 812-827 e819.

Li, Q., Nie, J., Wu, J., Zhang, L., Ding, R., Wang, H., Zhang, Y., Li, T., Liu, S., Zhang, M., *et al.* (2021). SARS-CoV-2 501Y.V2 variants lack higher infectivity but do have immune escape. Cell *184*,2362-2371.e9.

Li, Q., Wu, J., Nie, J., Zhang, L., Hao, H., Liu, S., Zhao, C., Zhang, Q., Liu, H., Nie, L., *et al.* (2020). The Impact of Mutations in SARS-CoV-2 Spike on Viral Infectivity and Antigenicity. Cell *182*, 1284-1294 e1289.

Liang, T., Cheng, M., Teng, F., Wang, H., Deng, Y., Zhang, J., Qin, C., Guo, S., Zhao, H., and Yu, X. (2021). Proteome-wide epitope mapping identifies a resource of antibodies for SARS-CoV-2 detection and neutralization. Signal Transduct Target Ther *6*, 166.

Liu, Y., Liu, J., Xia, H., Zhang, X., Fontes-Garfias, C.R., Swanson, K.A., Cai, H., Sarkar, R., Chen, W., Cutler, M., *et al.* (2021). Neutralizing Activity of BNT162b2-Elicited Serum. N Engl J Med *384*,1466-1468.

Madhi, S.A., Baillie, V., Cutland, C.L., Voysey, M., Koen, A.L., Fairlie, L., Padayachee, S.D., Dheda, K., Barnabas, S.L., Bhorat, Q.E., *et al.* (2021). Efficacy of the ChAdOx1 nCoV-19 Covid-19 Vaccine against the B.1.351 Variant. N Engl J Med, NEJMoa2102214.

Mercado, N.B., Zahn, R., Wegmann, F., Loos, C., Chandrashekar, A., Yu, J., Liu, J., Peter, L., McMahan, K., Tostanoski, L.H., *et al.* (2020). Single-shot Ad26 vaccine protects against SARS-CoV-2 in rhesus

macaques. Nature *586*, 583-588.

Muecksch, F., Weisblum, Y., Barnes, C.O., Schmidt, F., Schaefer-Babajew, D., Lorenzi, J.C.C., Flyak, A.I., DeLaitsch, A.T., Huey-Tubman, K.E., Hou, S., *et al.* (2021). Development of potency, breadth and resilience to viral escape mutations in SARS-CoV-2 neutralizing antibodies. bioRxiv.

Nie, J., Li, Q., Wu, J., Zhao, C., Hao, H., Liu, H., Zhang, L., Nie, L., Qin, H., Wang, M., *et al.* (2020). Quantification of SARS-CoV-2 neutralizing antibody by a pseudotyped virus-based assay. Nat Protoc *15*, 3699-3715.

Prevost, J., and Finzi, A. (2021). The great escape? SARS-CoV-2 variants evading neutralizing responses. Cell Host Microbe *29*, 322-324.

Priesemann, V., Balling, R., Brinkmann, M.M., Ciesek, S., Czypionka, T., Eckerle, I., Giordano, G., Hanson, C., Hel, Z., Hotulainen, P., *et al.* (2021). An action plan for pan-European defence against new SARS-CoV-2 variants. Lancet *397*, 469-470.

Singh, A., Steinkellner, G., Kochl, K., Gruber, K., and Gruber, C.C. (2021). Serine 477 plays a crucial role in the interaction of the SARS-CoV-2 spike protein with the human receptor ACE2. Sci Rep *11*, 4320.

Stamatatos, L., Czartoski, J., Wan, Y.H., Homad, L.J., Rubin, V., Glantz, H., Neradilek, M., Seydoux, E., Jennewein, M.F., MacCamy, A.J., *et al.* (2021). mRNA vaccination boosts cross-variant neutralizing antibodies elicited by SARS-CoV-2 infection. Science, eabg9175.

Starr, T.N., Greaney, A.J., Dingens, A.S., and Bloom, J.D. (2021). Complete map of SARS-CoV-2 RBD mutations that escape the monoclonal antibody LY-CoV555 and its cocktail with LY-CoV016. Cell Rep Med *2*,100255.

Starr., T., Czudnochowski., N., Zatta., F., Park., Y., Veesler., D., Corti., D., Bloom., J., and Snell., G. (2021). Antibodies to the SARS-CoV-2 receptor-binding domain that maximize breadth and resistance to viral escape. bioRxiv.

Tan, C.W., Chia, W.N., Qin, X., Liu, P., Chen, M.I., Tiu, C., Hu, Z., Chen, V.C., Young, B.E., Sia, W.R., *et al.* (2020). A SARS-CoV-2 surrogate virus neutralization test based on antibody-mediated blockage of ACE2-spike protein-protein interaction. Nat Biotechnol *38*, 1073-1078.

Wang, H., Wu, X., Zhang, X., Hou, X., Liang, T., Wang, D., Teng, F., Dai, J., Duan, H., Guo, S., *et al.* (2020). SARS-CoV-2 Proteome Microarray for Mapping COVID-19 Antibody Interactions at Amino Acid Resolution. ACS Cent Sci *6*, 2238-2249.

Wang, P., Nair, M.S., Liu, L., Iketani, S., Luo, Y., Guo, Y., Wang, M., Yu, J., Zhang, B., Kwong, P.D., *et al.* (2021a). Antibody Resistance of SARS-CoV-2 Variants B.1.351 and B.1.1.7. Nature *593*,130-135.

Wang, P., Wang, M., Yu, J., Cerutti, G., Nair, M.S., Huang, Y., Kwong, P.D., Shapiro, L., and Ho, D.D. (2021b). Increased Resistance of SARS-CoV-2 Variant P.1 to Antibody Neutralization. bioRxiv.

Wang., H., Hou., X., Zhang., X., Wu., X., Liang., T., Wang., D., Teng., F., Dai., J., Duan., H., Guo., S., *et al.* (2020). SARS-CoV-2 proteome microarray for mapping COVID-19 antibody interactions at amino acid resolution. ACS Cent Sci *6*,2238-2249.

Weisblum, Y., Schmidt, F., Zhang, F., DaSilva, J., Poston, D., Lorenzi, J.C., Muecksch, F., Rutkowska, M., Hoffmann, H.H., Michailidis, E., *et al.* (2020). Escape from neutralizing antibodies by SARS-CoV-2 spike protein variants. Elife *9*,e61312.

Wibmer, C.K., Ayres, F., Hermanus, T., Madzivhandila, M., Kgagudi, P., Oosthuysen, B., Lambson, B.E., de Oliveira, T., Vermeulen, M., van der Berg, K., *et al.* (2021). SARS-CoV-2 501Y.V2 escapes neutralization by South African COVID-19 donor plasma. Nat Med *27*,622-625..

Wu, Z., Hu, Y., Xu, M., Chen, Z., Yang, W., Jiang, Z., Li, M., Jin, H., Cui, G., Chen, P., *et al.* (2021). Safety, tolerability, and immunogenicity of an inactivated SARS-CoV-2 vaccine (CoronaVac) in healthy adults

aged 60 years and older: a randomised, double-blind, placebo-controlled, phase 1/2 clinical trial. Lancet Infect Dis,S1473-3099(20)30987-7.

Xu, M., Deng, J., Xu, K., Zhu, T., Han, L., Yan, Y., Yao, D., Deng, H., Wang, D., Sun, Y., *et al.* (2019). In-depth serum proteomics reveals biomarkers of psoriasis severity and response to traditional Chinese medicine. Theranostics *9*, 2475-2488.

Xu, M., Wang, D., Wang, H., Zhang, X., Liang, T., Zhang, K., Zhang, J., Xu, D., and Yu, X. (2020). COVID-19 diagnostic testing: Technology perspective. Clin Transl Med, e158.

Yu, J., Tostanoski, L.H., Peter, L., Mercado, N.B., McMahan, K., Mahrokhian, S.H., Nkolola, J.P., Liu, J., Li, Z., Chandrashekar, A., *et al.* (2020). DNA vaccine protection against SARS-CoV-2 in rhesus macaques. Science *369*, 806-811.

Zhang, L., Jackson, C.B., Mou, H., Ojha, A., Peng, H., Quinlan, B.D., Rangarajan, E.S., Pan, A., Vanderheiden, A., Suthar, M.S., *et al.* (2020a). SARS-CoV-2 spike-protein D614G mutation increases virion spike density and infectivity. Nat Commun *11*, 6013.

Zhang, N.N., Li, X.F., Deng, Y.Q., Zhao, H., Huang, Y.J., Yang, G., Huang, W.J., Gao, P., Zhou, C., Zhang, R.R., *et al.* (2020b). A Thermostable mRNA Vaccine against COVID-19. Cell *182*, 1271-1283 e1216.

Zhou, D., Dejnirattisai, W., Supasa, P., Liu, C., Mentzer, A.J., Ginn, H.M., Zhao, Y., Duyvesteyn, H.M.E., Tuekprakhon, A., Nutalai, R., *et al.* (2021). Evidence of escape of SARS-CoV-2 variant B.1.351 from natural and vaccine-induced sera. Cell *184*,2348-2361.

Contributions

J.Z. and L.X. provided the purified spike variant proteins. M. Z., S. Y., C. H., Y. H., and Y. W. provided the clinical samples. X. Z., H. W., J. Z., J. R., H. B., and X. Y. executed microarray experiments. X. Z., T. L., H. P., S. L., C.W., and X.Y. executed the bioinformatics and statistical analyses. J.V. executed the pseudovirus based neutralization assay. H. Z., M. L., X. H., and B. K. executed the authentic virus-based neutralization assay. X.Y., Y. W., and B. K. conceived the idea, designed experiments, analyzed the data, and wrote the manuscript.

Acknowledgement

This work was supported by the National Natural Science Foundation of China (31870823), National Key R&D Program of China (2020YFE0202200), State

Key Laboratory of Proteomics (SKLP-C202001, SKLP-O201904, SKLP-O201703, SKLP-O202007), the National Program on Key Basic Research Project (2018YFA0507503, 2017YFC0906703, 2018ZX09733003) and the Beijing Municipal Education Commission, Beijing Municipal Natural Science Foundation (M21003) and Beijing Municipal Science & Technology Commission (Z201100001020001; Z201100005420022). We thank Dr. Brianne Petritis for her critical review and editing of this manuscript.

Competing interests

None declared.

Supplemental information

The supplemental information includes 3 supplementary tables and 9 supplementary figures.

Figures and legends

Figure 1. Development of the mSAIS assay. (A) A schematic illustration of the microarray-based mSAIS assay and potential biomedical applications; (B, C) Intra- and inter-array reproducibility of the mSAIS assay in the absence and presence of neutralizing antibodies, respectively.

Figure 2. SARS-CoV-2 S-ACE2 interaction mapping across different S

variants using the mSAIS assay. (A) Detection of different concentrations of ACE2 binding to S variants immobilized on the array. (B) Distribution of S-ACE2 binding affinities (EC50) across different SARS-CoV-2 S variants. (C) Fold changes of binding affinity between the wild-type and mutated S proteins. The x-axis represents the S variants and the y-axis represents the log2 transformed IC50 ratio between the wild-type and mutated S proteins. (D) are the dynamic curves representing S variants that bind to ACE2 with significantly decreased binding affinity compared to the wild-type S protein. (E) Structural analysis of escape mutations on the RBD (gray color) that interacts with ACE2 (green color). RBD mutations (PDB ID: 6M0J) are labelled in red.

Figure 3. Heterogeneous responses of purified antibodies to SARS-CoV-2 mutations. (A-C) Distribution of neutralization activity (IC50) of purified antibodies #73, #21 and #53 to the S variants, respectively. The x-axis represents the S variants and the y-axis represents the neutralization activity (IC50) of the monoclonal antibody to each spike variant. (D, E) Fold changes of the neutralization activity (IC50) of antibodies #21 and #53 between the wild-type and mutant S proteins, respectively. The x-axis represents the S variants and the y-axis represents the log2 transformed IC50 ratio between the wild-type and mutated S proteins. (F, G) Structural analysis of the mutations that decrease and increase the neutralization activity of antibodies #21 and #53, respectively.

Figure 4. Heterogeneous responses of serological NAbs to SARS-CoV-2 S mutations in convalescent COVID-19 patients. (A) Hierarchical cluster analysis of NAbs to S variants in convalescent COVID-19 patients. The rainbow color from white to red correspond to the NAb titer from low to high, respectively. (B) EC50 comparison of convalescent COVID-19 patients with high and low NAb titers. (C) Comparison of escape mutations between convalescent COVID-19 patients with high and low NAb titers with EC50 thresholds set at 10, 30 and 50, respectively. (D) Distribution of serological NAbs to different SARS-CoV-2 S variants in convalescent COVID-19 patients. (E) Comparison of NAbs between the wild-type and D614G S proteins. (F) Comparison of NAbs between the wild-type S protein and S variants with known escape mutations. (G) Comparison of NAbs between the wild-type S protein and S variants with newly identified escape mutations. Significant escape mutations were identified using an unpaired t test with a p value of 0.05.

Figure 5. Heterogeneous responses of serological NAbs to the SARS-CoV-2 S mutations in vaccinated individuals. (A) Hierarchical cluster analysis of NAbs to S variants in vaccinees. The rainbow color from white to red correspond the NAb titers from low to high, respectively. (B) EC50 comparison of vaccinees with high and low NAb titers. (C) Comparison of

escape mutations between vaccinees with high and low NAb titers with EC50 thresholds set at 10, 20 and 30, respectively. (D) Distribution of serological NAbs to different SARS-CoV-2 S variants in vaccinees. (E) Comparison of NAbs between the wild-type and D614G S proteins. (F) Comparison of NAbs between the wild-type S protein and S variants with known escape mutations. (G) Comparison of NAbs between the wild-type S protein and S variants with newly-identified escape mutations. Significant escape mutations were identified using an unpaired t test with a p-value of 0.05. (H) Detection of serological NAbs to prevalent SARS-CoV-2 variants in the vaccinees using the pseudovirus neutralization assay. (I) Hierarchical cluster analysis of the NAbs to prevalent SARS-CoV-2 variants in vaccinees. The rainbow color from white to red correspond the NAb titers from low to high, respectively.

Figure 6. The NAb titer is associated with the diversity of anti-S antibodies in the serum of vaccinees. (A) A comparison of levels of antibodies that target the S1, RBD and S2 ECD. (B) Identification of vaccine-induced humoral immune responses to the S protein. (C) Association between the number of immunogenic peptides and NAb titers. A p-value (p) < 0.05 by Mann-Whitney test was considered to be significant. NTD = N-terminal domain

Figure 7. Validation of anti-S antibody diversity in 104 vaccinees. (A) A

589 comparison of levels of antibodies that target the S proteins and its domains.
590 (B) Landscape of vaccine-induced humoral immune responses to the S protein.
591 (C) Association between the number of immunogenic peptides and NAb titers.
592 A p-value (p) < 0.05 by Mann-Whitney test was considered to be significant.
593 CTD = C-terminal domain; NTD = N-terminal domain. The NAb titers (ND50)
594 was measured using pseudovirus neutralization assay.
595

596 ## Materials and methods

597 ### Collection of patient samples

598 Clinical specimens were obtained from the Department of Clinical Laboratory
599 in Beijing Ditan Hospital, Capital Medical University (Beijing, China). Whole
600 blood was collected in a vacutainer tube, and centrifuged at 4,000×g at room
601 temperature (RT) for 10 minutes to separate serum. Serum was then
602 transferred to a clean tube and stored at -80℃ until use. For safety purposes,
603 serum collected from convalescent COVID-19 patients was inactivated at 56℃
604 for 30 minutes prior to any further sample processing. Notably, serum from
605 COVID-19 vaccinated individuals was obtained from healthy hospital staff 4
606 weeks after receiving the second vaccine dose, and convalescent samples
607 were collected from COVID-19 patients 2 to 4 weeks post discharge. Our
608 research was approved by the Ethics Committee of Beijing Ditan Hospital (No.
609 2021-010-01), and exemption of informed consent was obtained prior to sera
610 collection.

611

612 **Expression and purification of recombinant proteins for use on the**
613 **mSAIS assay**

614 The DNA sequence encoding the SARS-CoV-2 Spike protein (S1+S2 ECD)
615 (YP_009724390.1) (Val 16-Pro1213), S1 Subunit (YP_009724390.1)
616 (Val16-Arg685), RBD (YP_009724390.1) (Arg319-Phe541) or variants were
617 expressed with a polyhistidine tag at the C-terminus. The generation of
618 variants using site-directed mutagenesis was performed as previously
619 described (Li et al., 2020). In addition, two negative controls [SARS-CoV-2
620 Nucleocapsid (N), MERS-CoV-2 Spike RBD], one positive control
621 (SARS-CoV-2 wild-type RBD), and the extracellular domain of ACE2 were
622 expressed with a polyhistidine tag at the C-terminus. The proteins were
623 expressed in HEK293 cells, followed by further purification on a Ni-NTA spin
624 column (Thermo Fisher). Protein purity was confirmed using an SDS-PAGE gel
625 stained with Coomassie blue.

626

627 **Preparation of the mSAIS microarray**

628 All purified proteins were diluted to 100 μg/mL and printed onto a
629 three-dimensional (3D)-modified slide surface (Capital Biochip Corp, Beijing,
630 China) in parallel and in duplicate using an Arrayjet microarrayer (Roslin, UK)
631 as previously described (Hou et al., 2020a; Wang et al., 2020; Xu et al., 2019).
632 The protein microarrays were stored at -20 ℃ until ready to use.

633

634 **Detection of NAbs using the mSAIS assay**

635 Prior to antibody detection, the protein microarrays were assembled in an
636 incubation tray and blocked with 1% (w/v) milk in 1x phosphate buffered saline,
637 pH 7.2 (PBS), with 0.2% (v/v) Tween-20 (PBST) for 10 min at room
638 temperature. After washing with PBST three times, the array was incubated
639 with serum diluted 10- to 320-fold in PBST for 30 min at room temperature.
640 After washing again, the array was then incubated for 60 min with Cy5-labeled
641 ACE2 (50 ng/mL). Finally, the array was washed with PBST and water,
642 dissembled from the tray, and dried via centrifugation for 2 min at 2,000 rpm.
643 The array was scanned with a GenePix 4300A microarray scanner (Molecular
644 Devices, Sunnyvale, CA, USA) at a 10 μm resolution using a laser at 635 nm
645 with 100% power/ PMT Gain 900. The median fluorescent signal intensity with
646 background subtraction was extracted using GenePix Pro7 software
647 (Molecular Devices, Sunnyvale, CA, USA).

648

649 **SARS-CoV-2 pseudovirus neutralization assay**

650 The SARS-CoV-2 pseudovirus neutralization assay was performed as
651 previously described (Nie et al., 2020). Briefly, human sera were diluted using
652 3-fold serial dilutions with a starting concentration of 1:10 (two per dilution).
653 The diluted sera were added into 96-well plates in duplicate, followed by the
654 SARS-CoV-2 pseudovirus at a concentration of 1300 median tissue culture

infective dose (TCID50/mL). The sera and pseudovirus were incubated together at 37℃ for 1 hour, and then monkey Vero cells were added at 2*10^4 cells/100 mL cells per well. The plates were incubated at 37℃ in a humidified atmosphere with 5% CO_2 for 24 hours before chemiluminescence detection was performed. The Reed-Muench method was used to calculate the neutralization titer.

Live SARS-CoV-2 neutralization assay

A suspension of Vero cells suspension was prepared at a cell density of 2×10^5/ml. Serum samples were diluted 4-fold in cell culture medium and inactivated at 56℃ for 30 minutes. The inactivated serum was serially diluted 2-fold with MEM medium, followed by the addition of cell culture medium containing 100 times the cell culture infective dose 50% (CCID50) of wild-type SARS-CoV-2 virus. The mixture was placed into a 96-well plate and incubated at 37°C for 2 h in CO_2 5%, and then 2×10^4 Vero cells were added and incubated again at 37°C. The samples were microscopically examined for cytopathic effect (CPE) after 7 days. The highest dilution of serum that showed complete inhibition activity of SARS-CoV-2 was recorded as the neutralizing antibody titer (ID50). Assays were performed in duplicate with negative control serum.

The ID50 was calculated as: LogCCID50 = Xm + 1/2d - d $\sum$pi/100, where Xm is the log10 of maximum dilution of the virus, the d is the logarithm of the

677 dilution fold, and ∑pi is the sum of the percentage of the cytopathic effect per
678 dilution.

679

680 **Detection of SARS-CoV-2 serum antibodies using a SARS-CoV-2**
681 **proteome peptide microarray**

682 The peptide microarray containing truncated S proteins, and tiled peptides
683 representing SARS-CoV-2 S protein was prepared as our previous work (Liang
684 et al., 2021; Wang. et al., 2020). The array was assembled in an incubation
685 tray and blocked with 5% (w/v) milk in phosphate-buffered saline (PBS)
686 containing 0.05% (v/v) Tween-20 (PBST) for 30 min at room temperature
687 before antibody detection. After aspirating the blocking solution, the 1:200
688 diluted serum was added to the array and incubated at room temperature for
689 20 min. After washing three times with PBST, the array was then incubated for
690 20 min with a Cy3 labelled donkey anti-human IgG(H+L) antibody (Jackson
691 ImmunoResearch, USA) (2 μg/mL). Finally, the array was washed with PBST
692 and deionized water, disassembled from the tray and dried with vacuum pump.
693 The slide was scanned at 532 nm using a GenePix 4300A microarray scanner
694 (Molecular Devices, Sunnyvale, CA, USA). The median fluorescent signal
695 intensity of each spot with background subtraction was extracted using
696 GenePix Pro7 software (Molecular Devices, Sunnyvale, CA, USA).

697

698 **Data analysis**

699 The ability of the serological NAbs to inhibit the S-ACE2 interactions across
700 the different S variants was visualized as a heatmap using the MultiExperiment
701 Viewer software version 4.9 (Chu et al., 2008). Statistical analyses were
702 performed using the GraphPad Prism software 8.3 and Microsoft Excel with
703 the unpaired t test and Mann-Whitney test. A p-value (p) < 0.05 was
704 considered to be significant. *$p < 0.05$, **$p < 0.01$, ***$p < 0.005$, ****$p < 0.001$.
705 The 3D structure of the SARS-CoV-2 RBD and ACE2 complex (PDB ID code:
706 6M0J) was visualized using the VMD 1.9.3, and mutations were annotated.

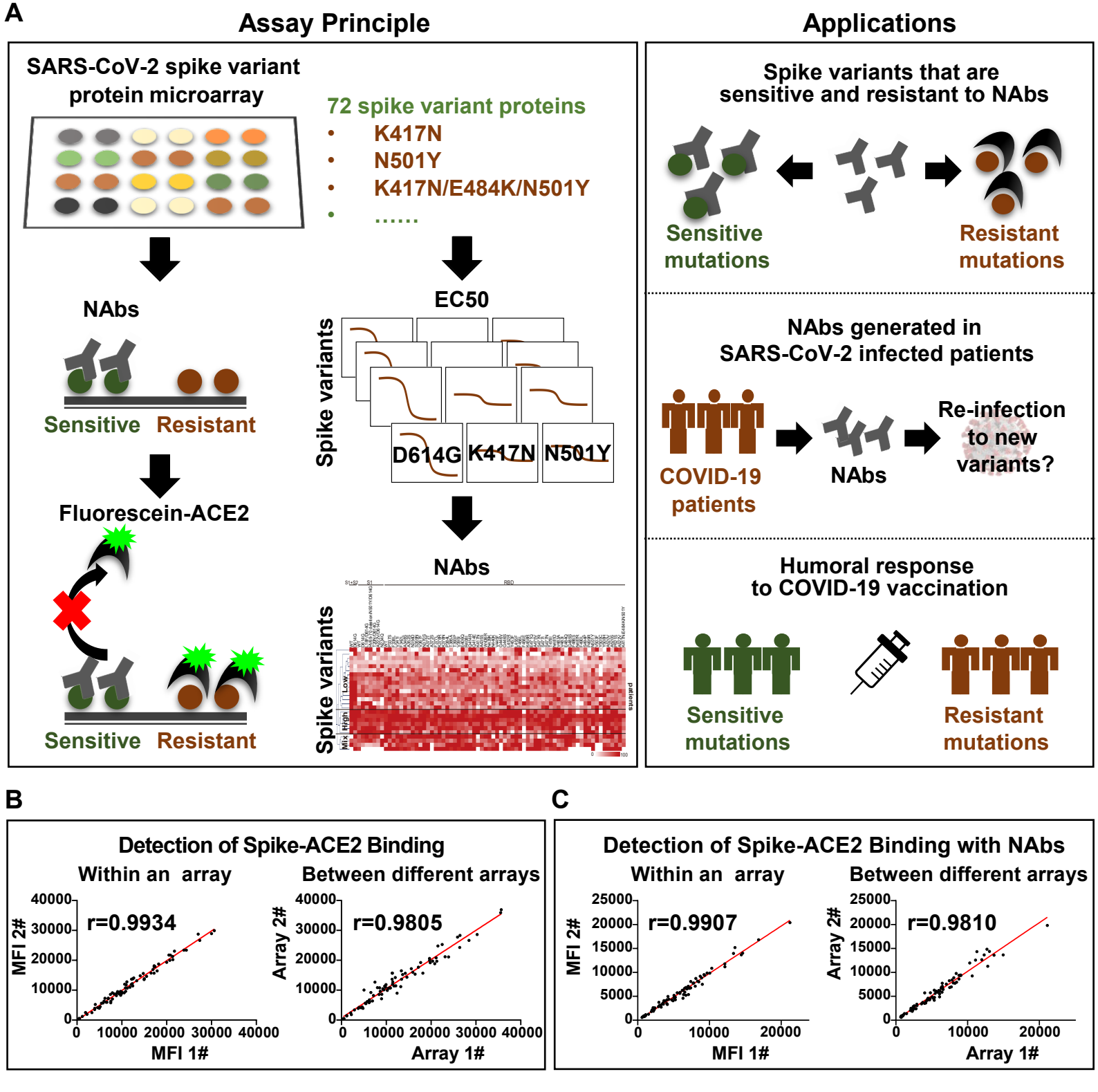
A
Assay Principle
Applications
SARS-CoV-2 spike variant protein microarray
72 spike variant proteins
K417N
N501Y
K417N/E484K/N501Y
.....
NAbs
Sensitive
Resistant
Fluorescein-ACE2
Sensitive
Resistant
EC50
Spike variants
D614G
K417N
N501Y
NAbs
Spike variants
Spike variants that are sensitive and resistant to NAbs
Sensitive mutations
Resistant mutations
NAbs generated in SARS-CoV-2 infected patients
COVID-19 patients
NAbs
Re-infection to new variants?
Humoral response to COVID-19 vaccination
Sensitive mutations
Resistant mutations
B
Detection of Spike-ACE2 Binding
Within an array
r=0.9934
MFI 2#
MFI 1#
Between different arrays
r=0.9805
Array 2#
Array 1#
C
Detection of Spike-ACE2 Binding with NAbs
Within an array
r=0.9907
MFI 2#
MFI 1#
Between different arrays
r=0.9810
Array 2#
Array 1#

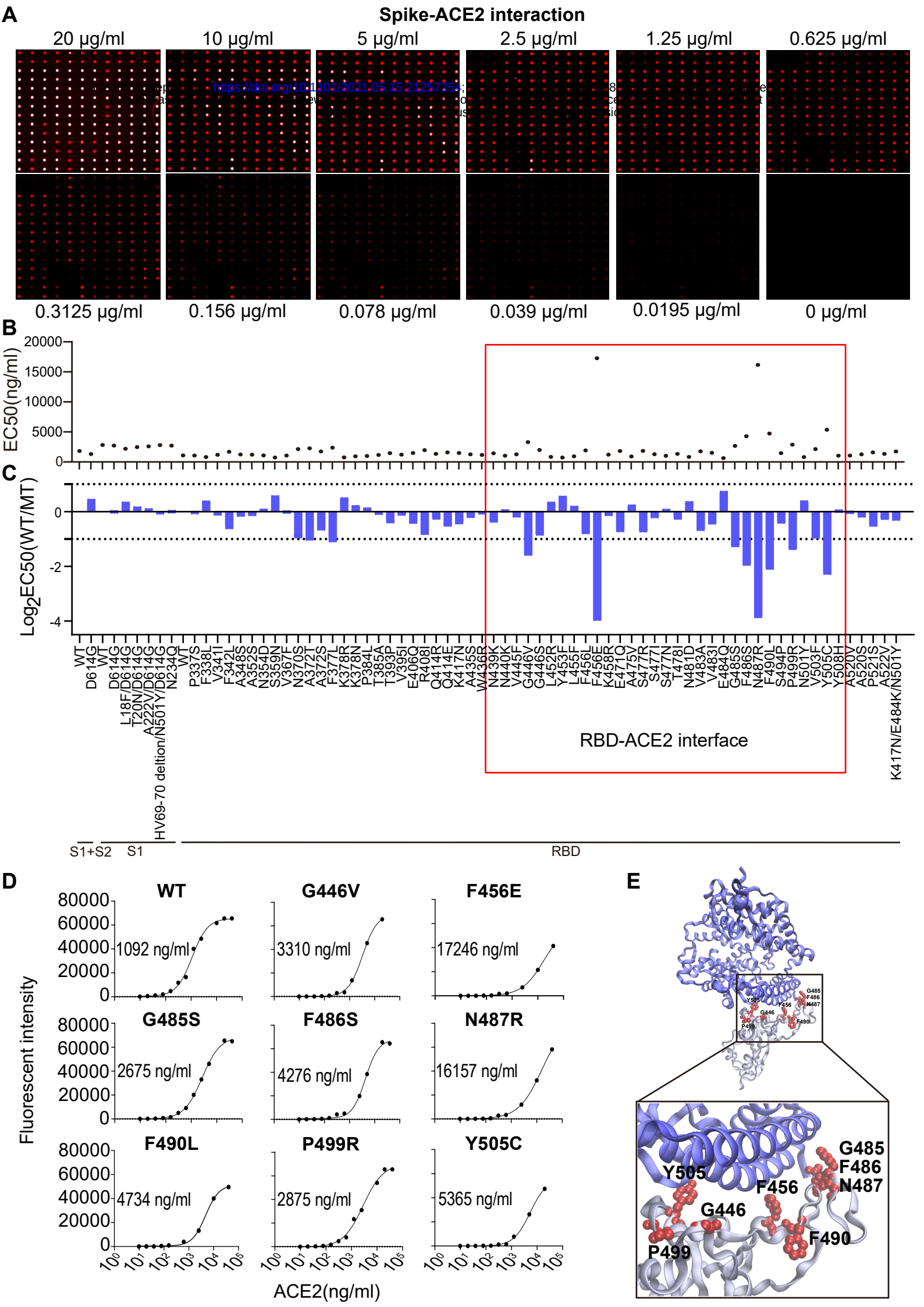
A
Spike-ACE2 interaction
20 μg/ml
10 μg/ml
5 μg/ml
2.5 μg/ml
1.25 μg/ml
0.625 μg/ml
0.3125 μg/ml
0.156 μg/ml
0.078 μg/ml
0.039 μg/ml
0.0195 μg/ml
0 μg/ml
B
EC50(ng/ml)
C
Log2EC50(WT/MT)
RBD-ACE2 interface
S1+S2
S1
RBD
D
WT
G446V
F456E
G485S
F486S
N487R
F490L
P499R
Y505C
1092 ng/ml
3310 ng/ml
17246 ng/ml
2675 ng/ml
4276 ng/ml
16157 ng/ml
4734 ng/ml
2875 ng/ml
5365 ng/ml
Fluorescent intensity
ACE2(ng/ml)
E
Y505
F456
G446
P499
G485
F486
N487
F490

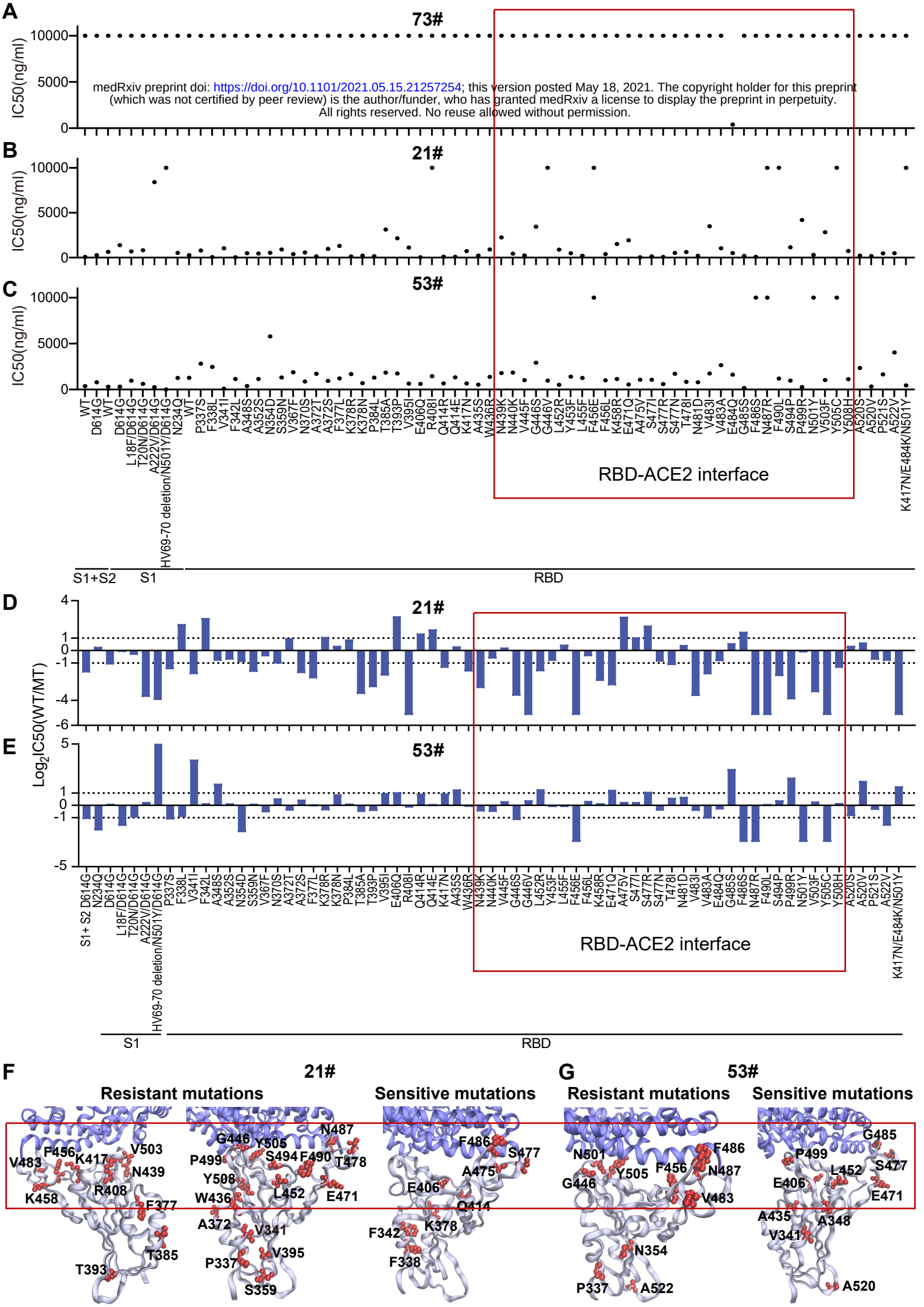

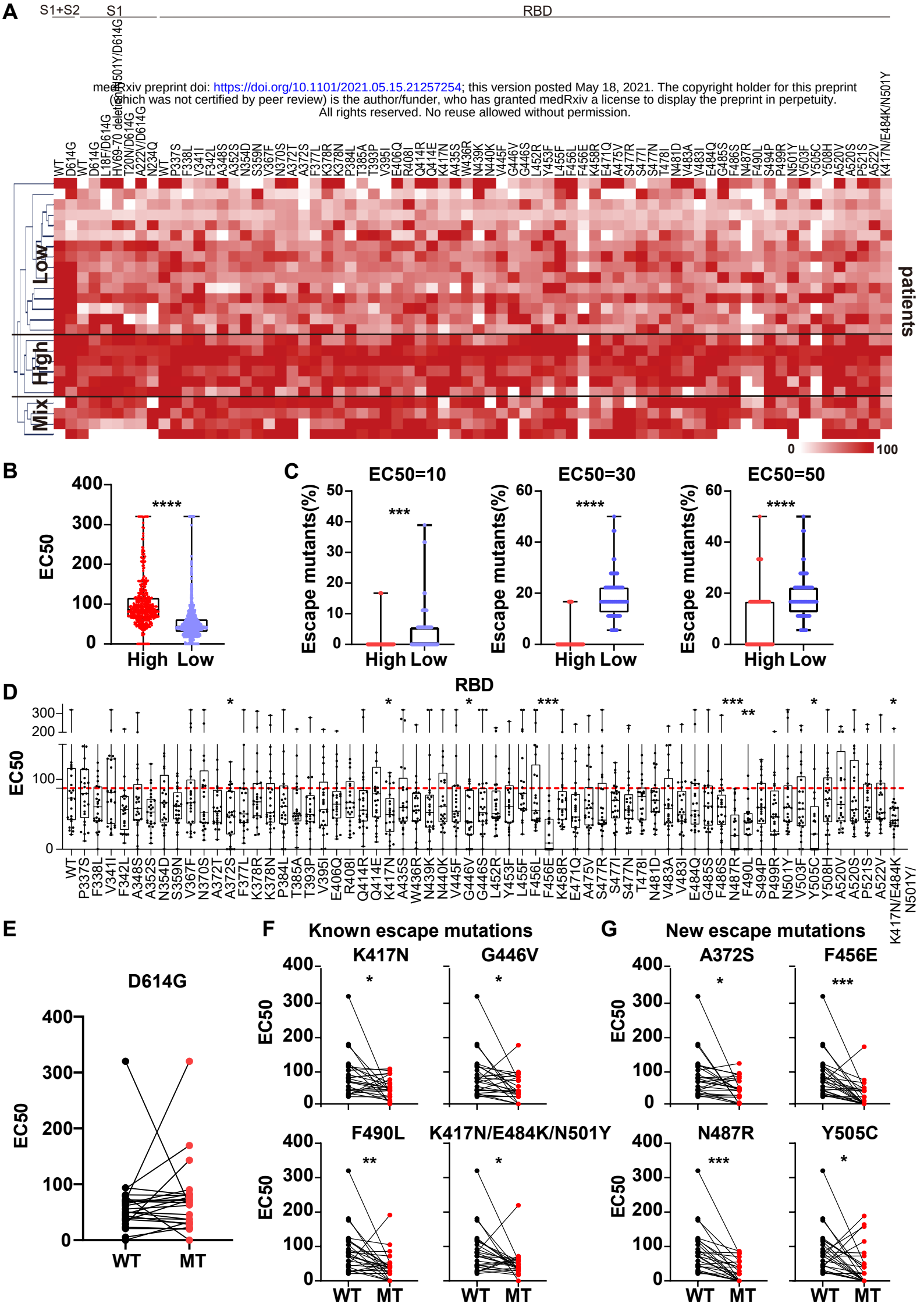

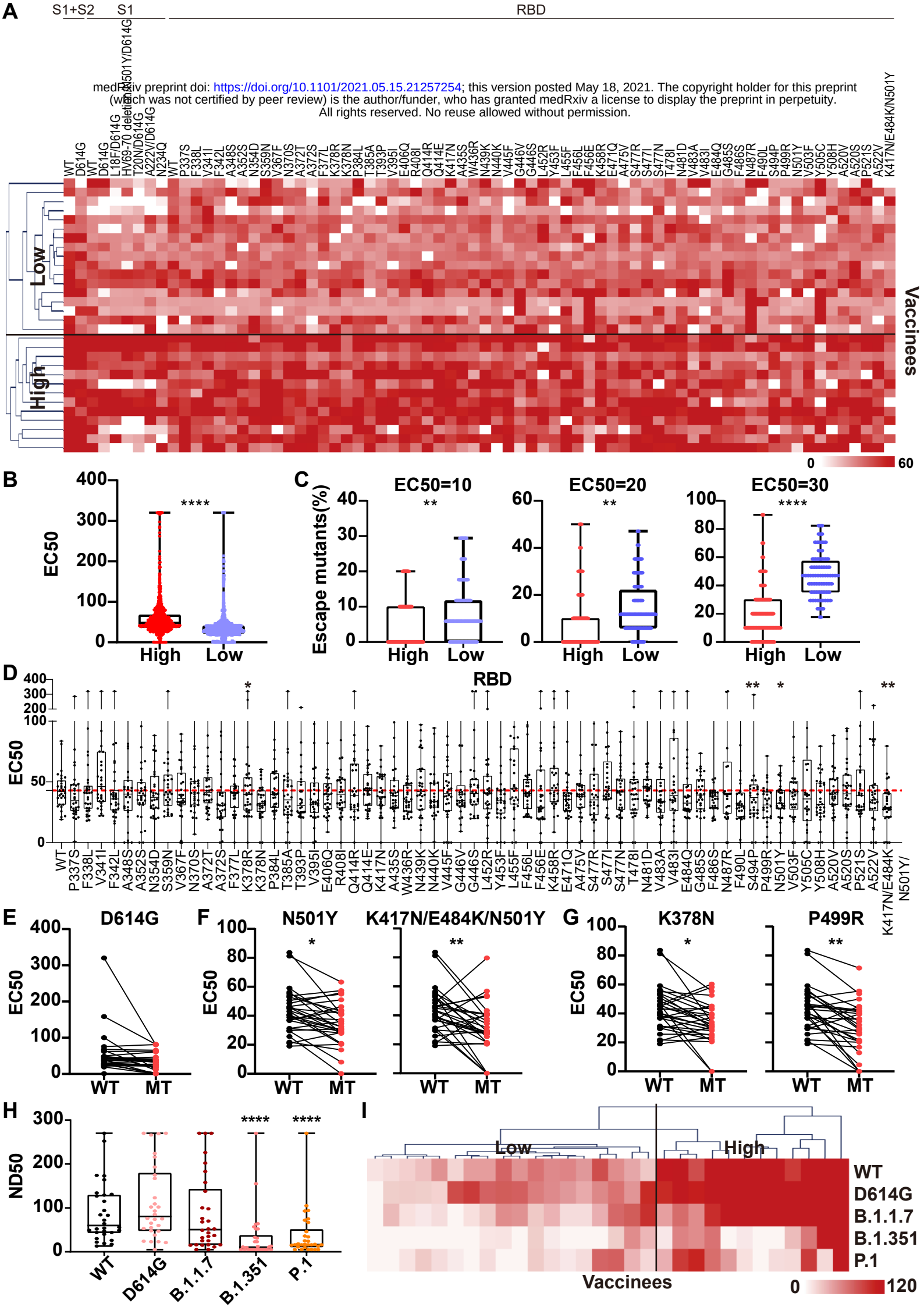

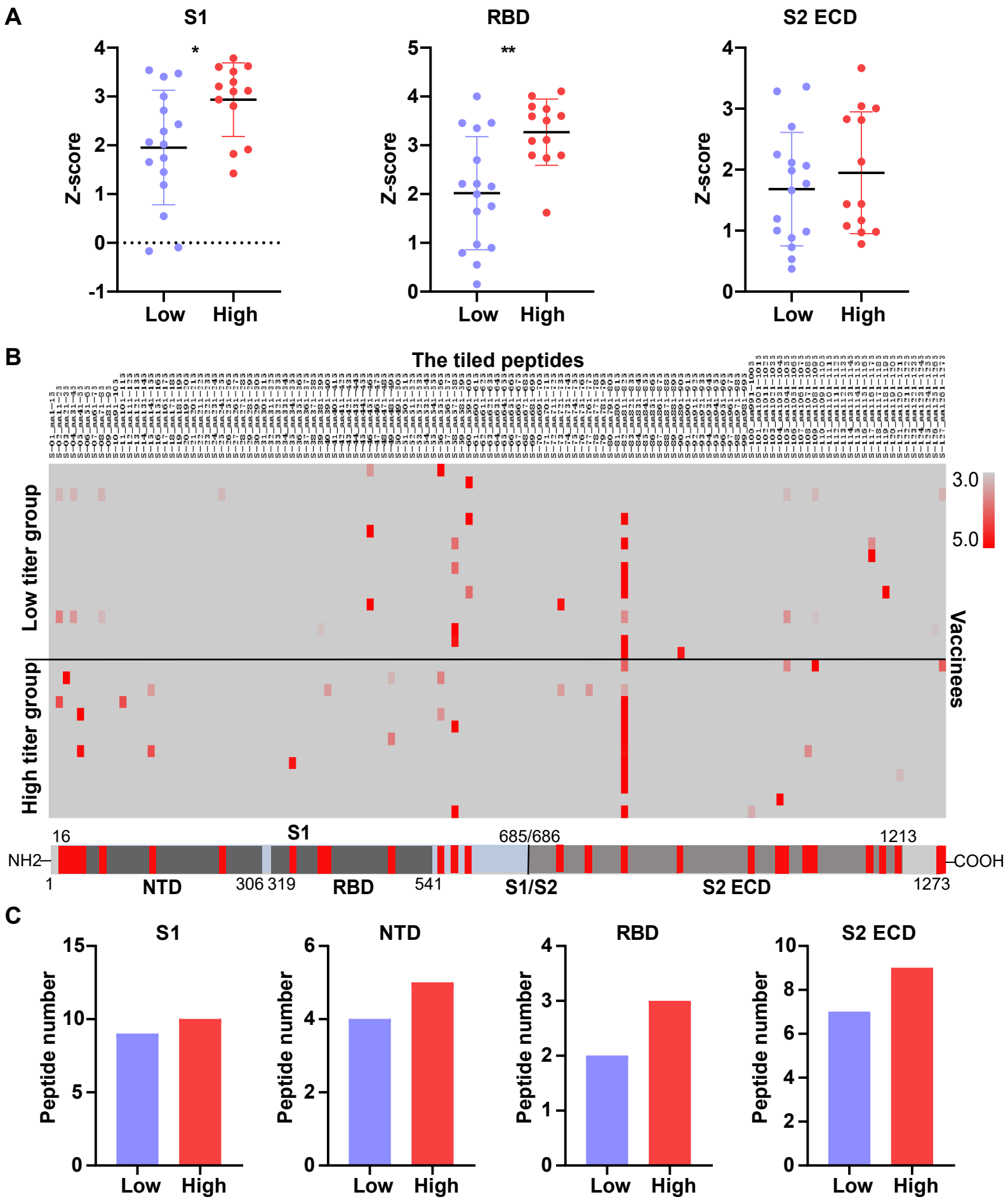
A
S1
RBD
S2 ECD
Z-score
Low
High
*
**
B
The tiled peptides
Low titer group
High titer group
Vaccinees
3.0
5.0
16
S1
685/686
1213
NH2
COOH
1
NTD
306 319
RBD
541
S1/S2
S2 ECD
1273
C
S1
NTD
RBD
S2 ECD
Peptide number
Low
High